SUPPLEMENTARY INFORMATION

Supplementary methods

1. PCR amplification and high-throughput sequencing

Bacterial DNA was extracted using the Qiagen DNeasy® Blood & Tissue Kit and the standard protocol designed for purification of total DNA from Gram-positive bacteria (Qiagen, Venlo, Netherlands). The V5-V6 region of the bacteria 16S rRNA gene was amplified by PCR using the following universal primers: BACTB-F: 5'-GGATTAGATACCCTGGTAGT-3' and BACTB-R: 5'-CACGACACGAGCTGACG-3' (1). To discriminate samples after sequencing, both forward and reverse primers were labelled at the 5' end with a combination of two different 8 bp tags. The PCR amplification was performed in a 25µL mixture containing 3µL of 1/10 diluted DNA extract, 0.4µM of each primers, 1U of AmpliTaq Gold DNA Polymerase (Applied Biosystems, Foster City, CA, USA), 1X of Taq Buffer, 0.24µL of bovine saline albumin (Promega Corporation, Madison, USA), 0.2mM of each dNTP, 2.5mM $MgCl_2$ and 12.06µL water and following this programme: initial denaturation at 95°C for 10min, 35 cycles of denaturation at 95°C for 30s, hybridation at 57°C for 30s and elongation at 72°C for 30s. All this lab work was done under sterile condition under laminar flux, all materials cleaned with ethanol and sterilized by UV light for 30min. In addition to biological samples, we also used negative and positive controls to check for the PCR effectiveness. PCR products were tested on electrophoresis gel and then 4 µL of amplicons per sample were pooled. The library construction (kit Illumina Biooscientific PCR free) and the sequencing (Illumina MiSeq 250 bp paired-end v3 chemistry) were performed at the Genopole of Toulouse (France).

2. Bioinformatic analysis

Illumina sequencing data were processed and filtered using the OBITools package. First, we aligned paired-end reads in consensus sequences by taking into account the reads overlapping quality and kept consensus reads with overlapping quality higher than 50. Second, we assigned reads to their respective sample by allowing zero error in tags and a maximum of two errors on primers. We further excluded reads containing ambiguous bases (other than A, T, G, C) and reads shorter than 100 bp as they are most likely sequencing errors (2). Remaining reads were then dereplicated and reads that occur only once in the entire dataset (singleton) were removed. Reads were then clustered into OTUs (Operational Taxonomic Unit) using SWARM algorithm with a similarity threshold of 97% of similarity (3). The most abundant sequence of each cluster was considered as the main sequence of this cluster and the representative sequence for the OTU. The taxonomic assignation was then performed on FROGS (Finding Rapidly Otu with Galaxy Solution), a Galaxy pipeline. The taxonomic affiliation was done by BLAST using the SILVA 132-16S gene data bank (4).

After taxonomic assignation, we obtained 5324394 sequences distributed along 282 OTUs with on average 5830±103SE sequences by samples (rarefaction curves in FIG. S2). We then applied different filters. We first identified contaminant OTUs (i.e. bacteria that did not come from the biological sample but from extraction or PCR reagents, or technical contamination during lab work) as OTUs with a higher maximum abundance and a higher mean abundance in negative controls than in biological samples. 96 OTUs (7.2% of the initial abundance) were identified as contaminant using these critera and then removed from the dataset. We then removed singleton OTUs and OTUs with a total abundance lower than 0.005% of the dataset's total abundance (2).

Inferred functional potential of bacterial communities were analyzed using PICRUSt. As the proportion of the sequences that failed to match the Greengenes reference was relatively high at the 97% similarity threshold (14% of the sequences were discarded), we used a 94% threshold leading to a less stringent but more comprehensive (only 2.4% of the sequences discarded). The average NSTI (Nearest Sequenced Taxon Index) value for the cloacal bacterial communities was 0.048±0.032, indicating a good coverage (5).

3. Statistical analyses

Diversity indexes were log-transformed to fit a normal distribution and were tested with generalised linear mixed effect models. To control for the differences in absolute abundance between samples (number of reads per samples), we used this sequencing depth as covariable in all the linear models used. Body condition was estimated using the scaled mass index (SMI, see 6) and individual mass gain or loss during the experiment was calculated by subtracting the mass at the end of the diet experiment by the mass recorded upon capture. Variation in α-diversity were first analysed using a global model including time (pre- versus post-experiment), diet, origin as fixed effects and bird ID and capture site as random effects. In a second stage, to specifically test for urbanisation and experimental diet effects, models were respectively subdivided in pre- and post-experiment as follows. Pre-experimental variation in α-diversity was analysed with models containing sex, age, SMI and origin (urban *vs.* rural birds) as fixed effects, sequencing depth as covariable and capture site as random effect. Post-experimental variation was analysed with models containing sex, age, SMI, origin and diet treatment as fixed effects, sequencing depth as covariable and cage ID as random effect. Variation in SMI pre- and post-experiment as the variation in mass gain were analysed with models containing sex, age, origin, diet treatment, the α-diversity indexes

(OtuRichness, Chao1 and Shannon index) at capture, sequencing depth as covariable and cage ID and bird ID as random effect. A minimal model containing only significant variables was selected through backward elimination of all non-significant variables (R package nlme), thus covariables such as sex and age are only mentioned when significant in the Results section. Inferred functional potential were analysed using STAMP (7), by comparing gene abundances with a Welch's t-test including Benjamin-Hochberg correction and using generalised linear mixed effect models containing sex, age, SMI, origin and diet treatment as fixed effects, sequencing depth as covariable and cage ID as random effect. To determine the contribution of β-diversity to changes in body mass in relation to the experimental diets, we included the first 2 principal coordinates of the pre-experimental PCoA in the mixed models explicited above.

Microbiota β-diversity was initially estimated using Jaccard (based on presence/absence community matrices), Bray-Curtis (based on relative abundance matrices after Hellinger transformation) and Unifrac dissimilarity distances. As the phylogenetic tree reconstructed based on the sequences only poorly recapitulated our taxonomic assignation (likely due the fact the V5-V6 region is short and fairly conserved), we had low confidence in the robustness of the tree and thus chose not to retain Unifrac as a metric of β-diversity. The effect of captivity (pre- vs post-experiment), diet treatment and origin and their interactions on the variance partitioning of dissimilarity was performed using Permutational Multivariate Analysis of Variance using the adonis2 function with 1000 permutations and using the option by="margin" to account to the effect of the different variables used in the model. Because differences in taxonomic composition were analyzed at the family level (see LDA analyses), we verified the congruence of PERMANOVA results based on family-binned matrices (Table S2). Inter-group dissimilarities were analysed with linear models including all pairwise

Jaccard distances between the different diet-origin combinations. To determine the contribution of β-diversity to changes in body mass in relation to the experimental diets, we included the first 2 principal coordinates of the pre-experimental PCoA in the mixed models explicited in the previous section. All analyses were performed with R using the VEGAN package. As Jaccard and Bray-Curtis distances yielded similar results, thus indicating that relative abundances do not contribute much to β-diversity in our dataset, only results using Jaccard distances are shown.

As a complementary approach to Linear Discriminant Analyses (see Methods section) to analyses differences in taxonomic composition, we used a compositional balance selection algorithm (R package selbal 8) in order to identify groups of microbial taxa that were predictive of urban and rural free-ranging sparrows.

Supplementary results

Effect of captivity on the gut microbiota

The six weeks of the diet experiment induced gut microbiota modification independently to the diet treatment. First, we observed an increase in α-diversity with an increase of the OTU richness and the Chao1 index at the end of the experiment (OTURichness, $F_{1,82}$=48.9, *p<0.0001*, mean capture=38.2±1.3, mean post-experiment=51±1.3, Chao $F_{1,77}$=13.9, *p=0.0004, Fig. S2*) but no significant change in the Shannon index ($F_{1,82}$=0.54, *p=0.47*). Secondly, the experiment resulted in significant shifts in gut microbiota composition (Table S1). Moreover, inter-host similarity significantly increased over the course of the experiment (GLMM: $F_{1,18}$=18.15, *p*<0.0001, mean capture=25.19±2.57, mean post-experiment=40.18±2.57). Third, gut microbiomes shifted in taxonomic composition compared to the original signature (Fig. S3). Finally, experimental treatment resulted in

fewer metabolic functions related to vitamin-, energy- and amino acid metabolism and a higher abundance of carbohydrate-,xenobiotics- and lipid metabolism (Welch's t-test, corrected p-value < 0.0001 for all above features, Fig. S4).

References

1. Fliegerova K, Tapio I, Bonin A, Mrazek J, Callegari ML, Bani P, et al. Effect of DNA extraction and sample preservation method on rumen bacterial population. Anaerobe. 2014 Oct 1;29:80–4.

2. Bokulich NA, Subramanian S, Faith JJ, Gevers D, Gordon JI, Knight R, et al. Quality-filtering vastly improves diversity estimates from Illumina amplicon sequencing. Nat Methods. 2013 Jan;10(1):57–9.

3. Mahé F, Rognes T, Quince C, Vargas C de, Dunthorn M. Swarm: robust and fast clustering method for amplicon-based studies. PeerJ. 2014 Sep 25;2:e593.

4. Camacho C, Coulouris G, Avagyan V, Ma N, Papadopoulos J, Bealer K, et al. BLAST+: architecture and applications. BMC Bioinformatics. 2009;10:421.

5. Langille MGI, Zaneveld J, Caporaso JG, McDonald D, Knights D, Reyes JA, et al. Predictive functional profiling of microbial communities using 16S rRNA marker gene sequences. Nat Biotechnol. 2013 Sep;31(9):814–21.

6. Peig J, Green AJ. New perspectives for estimating body condition from mass/length data: the scaled mass index as an alternative method. Oikos. 2009 Dec 1;118(12):1883–91.

7. Parks DH, Tyson GW, Hugenholtz P, Beiko RG. STAMP: statistical analysis of taxonomic and functional profiles. Bioinformatics. 2014 Nov 1;30(21):3123–4.

8. Rivera-Pinto J, Egozcue JJ, Pawlowsky-Glahn V, Paredes R, Noguera-Julian M, Calle ML. Balances: a New Perspective for Microbiome Analysis. mSystems [Internet]. 2018 Aug 28 [cited 2019 Nov 14];3(4). Available from: https://msystems.asm.org/content/3/4/e00053-18

Supporting Figures

origin	urban	rural	urban	rural	urban	rural	urban	rural	urban	rural	urban	rural	urban	rural	urban	rural	urban	rural	urban	rural	urban	rural	urban	rural
capture site	Pau	Cologne	Toulouse	Bourgezes	Tarbes	Montégut	Pau	Cologne	Toulouse	Bourgezes	Tarbes	Montégut	Pau	Cologne	Toulouse	Bourgezes	Tarbes	Montégut	Pau	Cologne	Toulouse	Bourgezes	Tarbes	Montégut
experimental diet	urban	urban	rural	rural	urban	urban	rural	rural	urban	urban	rural	rural	urban	urban	rural	rural	urban	urban	rural	rural	urban	urban	rural	rural
cage ID	1	2	3	4	5	6	7	8	9	10	11	12	13	14	15	16	17	18	19	20	21	22	23	24
nbr of birds	4	4	5	5	4	6	5	4	5	5	4	6	4	5	5	5	4	6	4	4	4	5	4	6

Figure S1 : Experimental design of the diet experiment

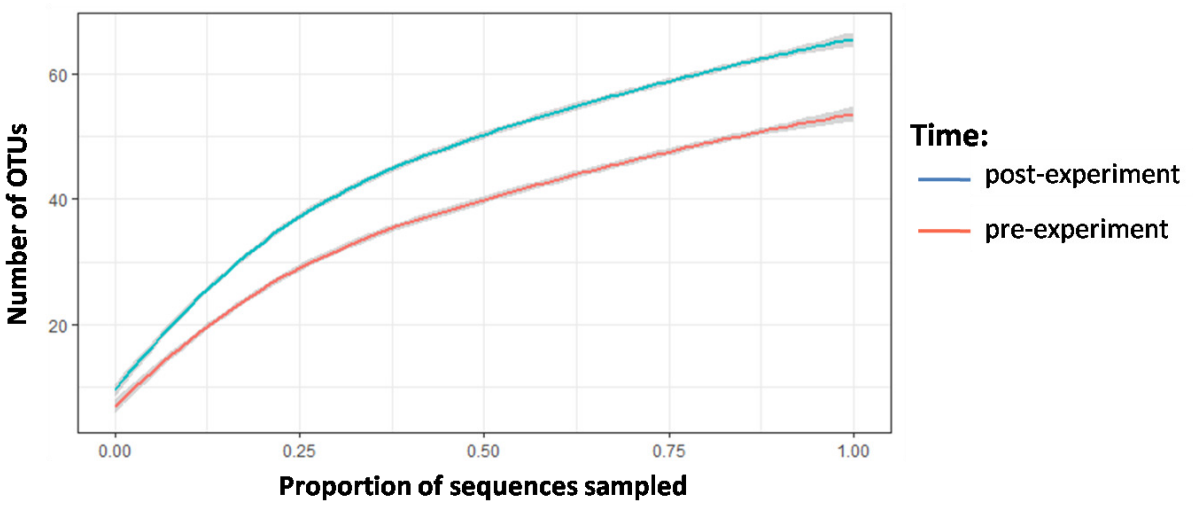

Figure S2 : Rarefaction curve of OTU richness with increasing number of sequences sampled according to time (pre-experiment vs. post-experiment)

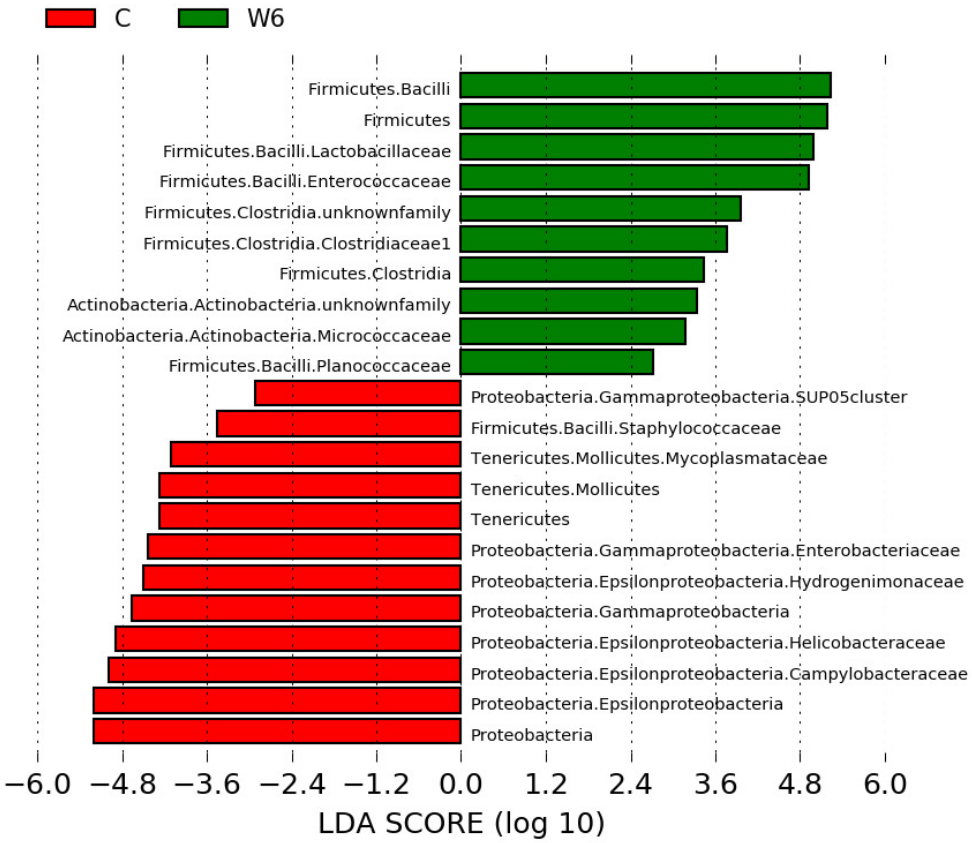

Figure S3: Linear Discriminant Analysis (LDA) of the change in taxonomic composition between the capture and the end of the experiment. Red and green colours represent taxa with significantly higher abundance at capture (C) or at the end of the experiment (W6) respectively.

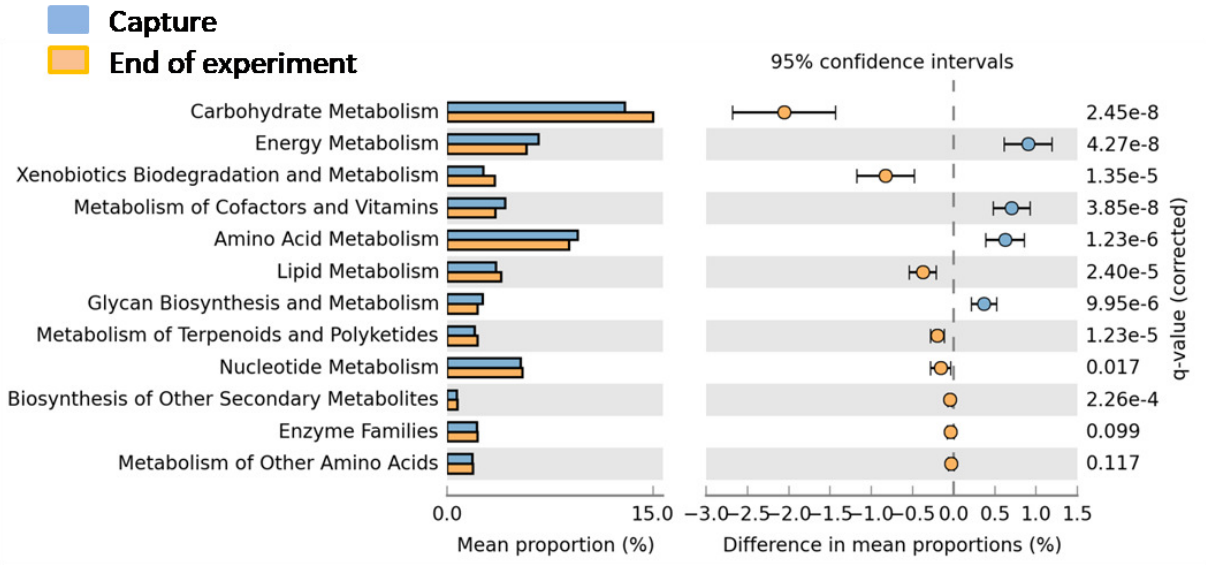

Figure S4: Mean proportion (%) and the difference in the mean proportion (%) of predicted and significantly different KEGG2 metabolic functional inferences of house sparrows along the diet experiment.

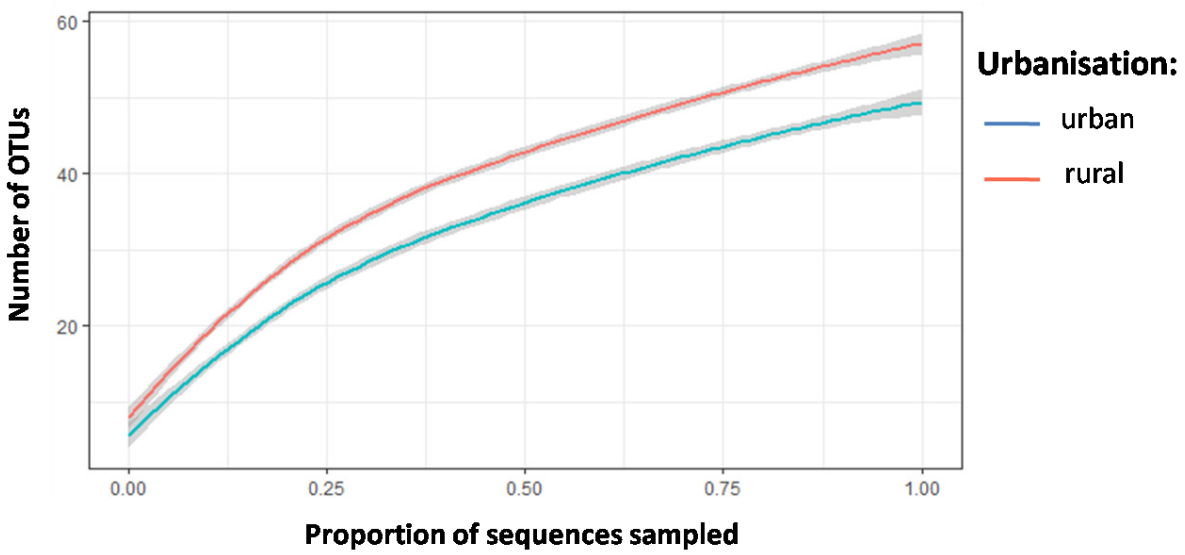

Figure S5 : Rarefaction curve of the number of OTUs with increasing number of sequences sampled in free-ranging birds according to their origin.

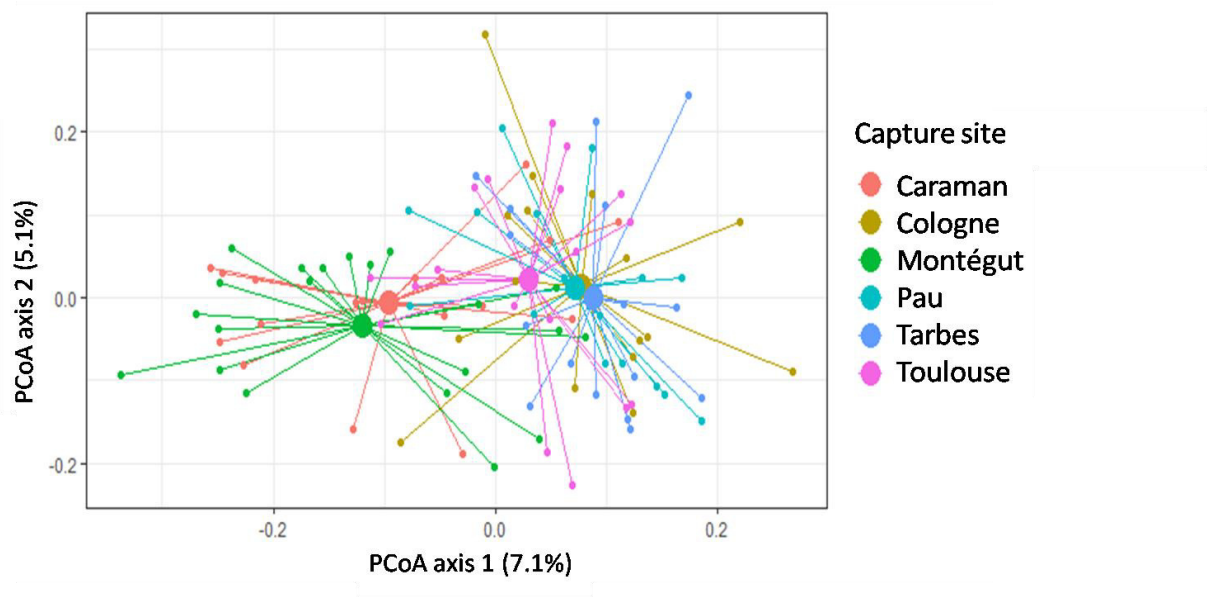

Figure S6: PCoA ordination based on a presence–absence similarity matrix of the gut microbiota of free-ranging house sparrows according to the capture sites. Numbers in parenthesis refer to the variance explained by the ordination axis.

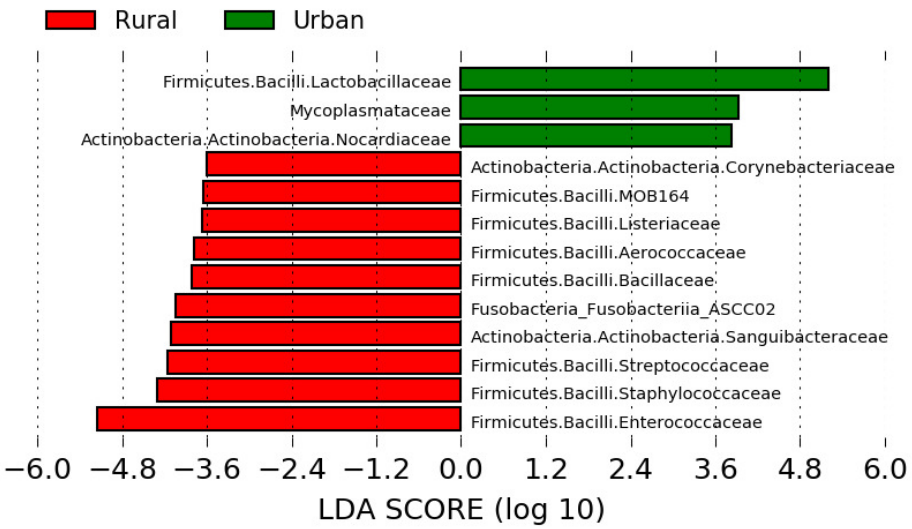

Figure S7: Linear Discriminant Analysis (LDA) of the gut microbiota taxa between urban and rural populations at capture. Red and green colours represent taxa with significantly higher abundance in rural or urban habitats respectively.

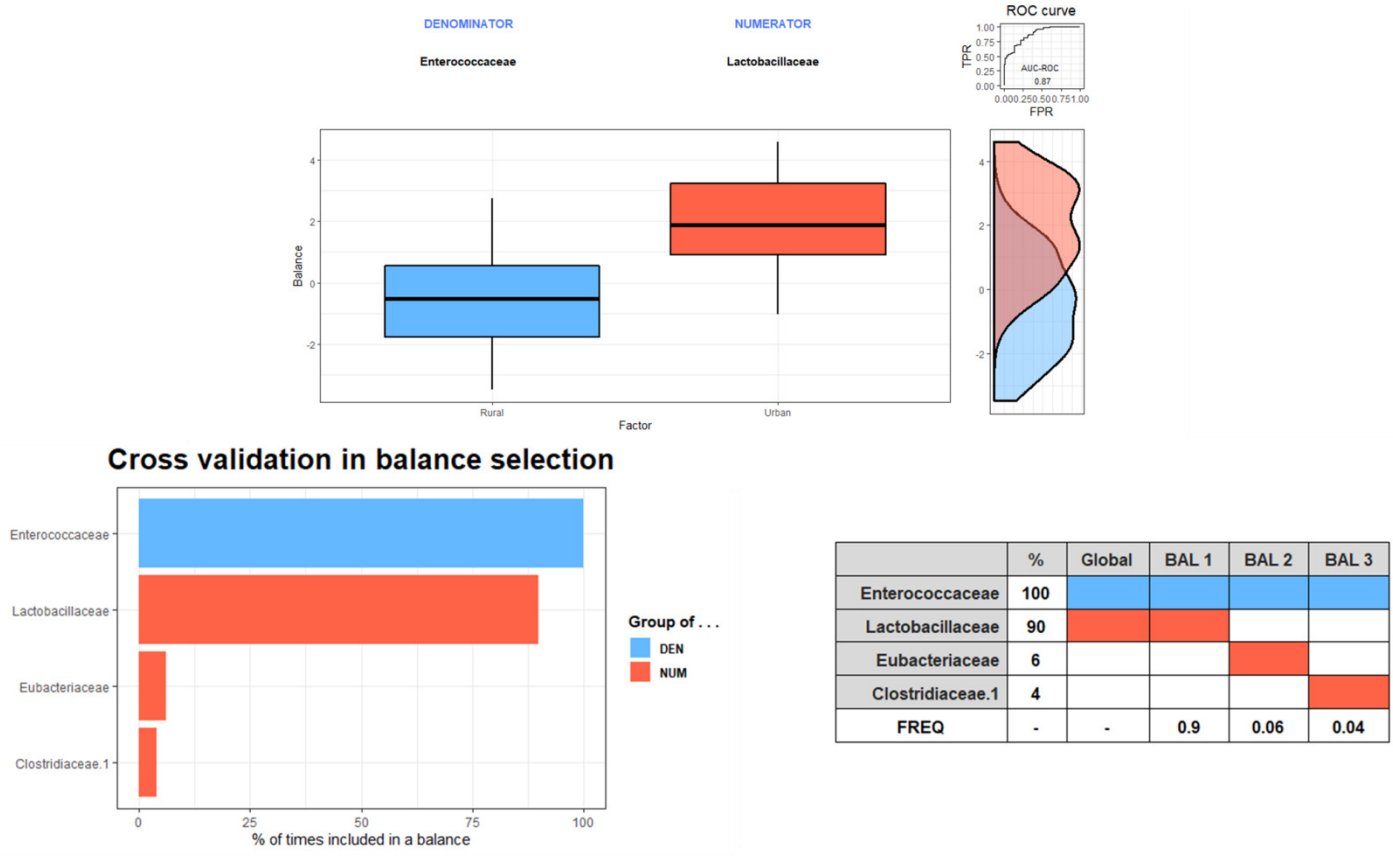

	%	Global	BAL 1	BAL 2	BAL 3
Enterococcaceae	100				
Lactobacillaceae	90				
Eubacteriaceae	6				
Clostridiaceae.1	4				
FREQ	-	-	0.9	0.06	0.04

Figure S8: Results of compositional balance selection approach to determine taxonomic microbial signatures. The taxa most predictive of the rural environment (denominator, blue colour) and urban environment (numerator, red colour) were respectively Enterococcaceae and Lactobacillaceae.

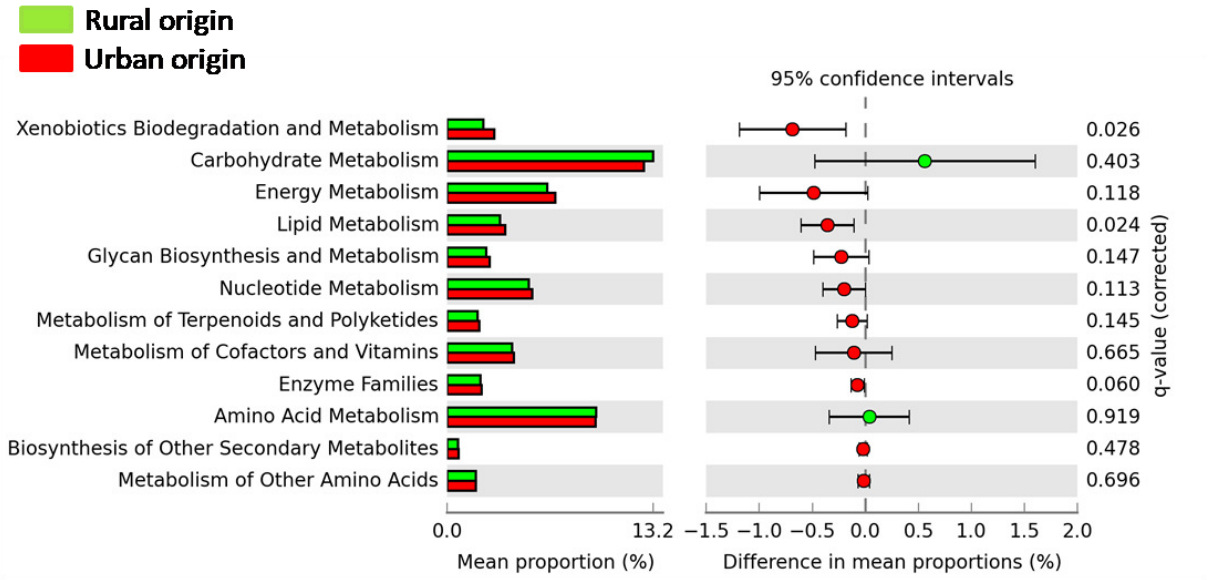

Figure S9: Mean proportion (%) and the difference in the mean proportion (%) of predicted and significantly different KEGG2 metabolic functional inferences of house sparrows according to the urbanisation of their capture sites.

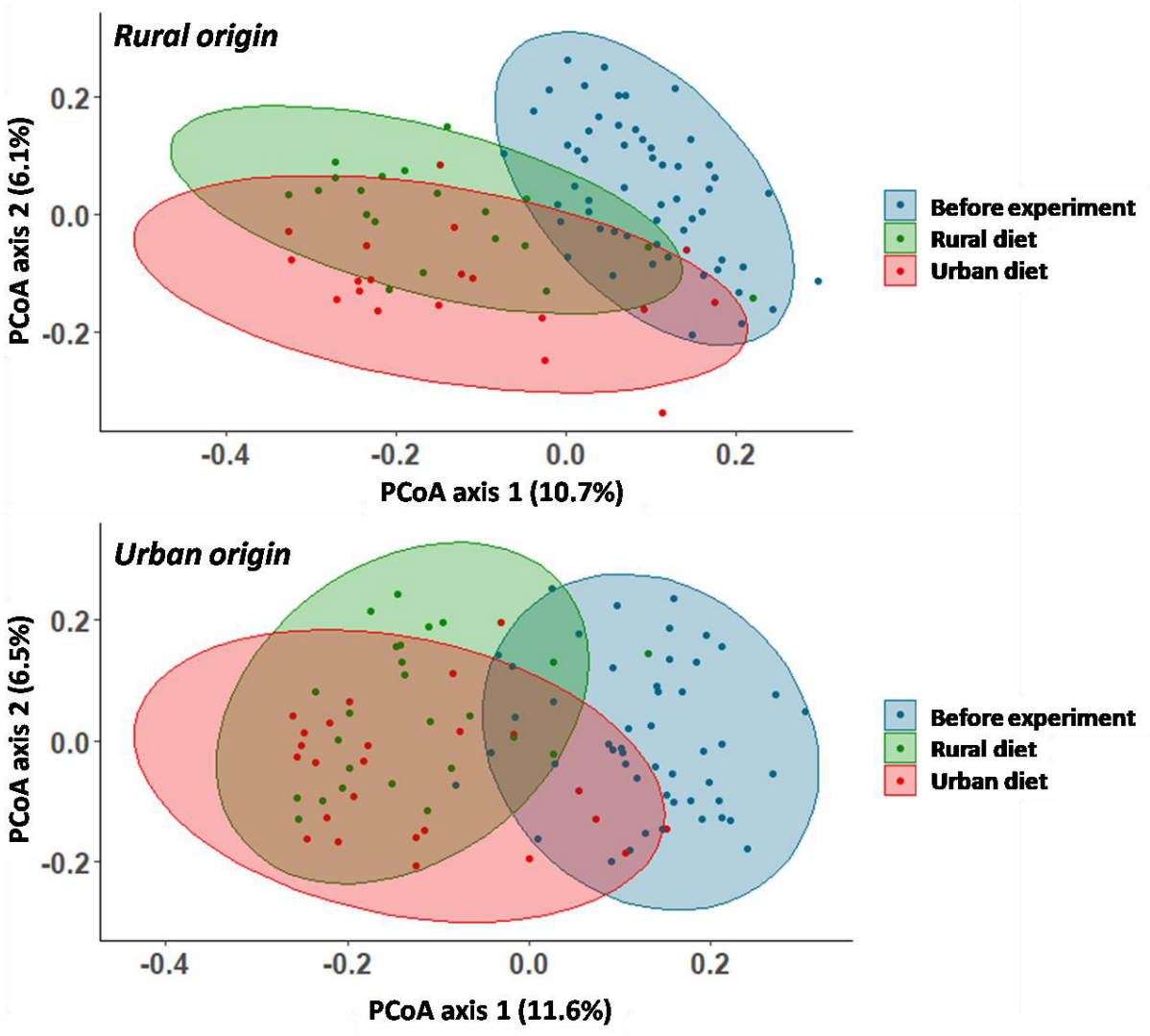

Figure S10: PCoA ordination based on presence–absence similarity matrices comparing microbiota of rural and urban birds, respectively, before experiment to post-experimental microbiota after exposure to the experimental diet. Numbers in parenthesis refer to the variance explained by the ordination axis. Coloured circles refer to 95% confident interval ellipses.

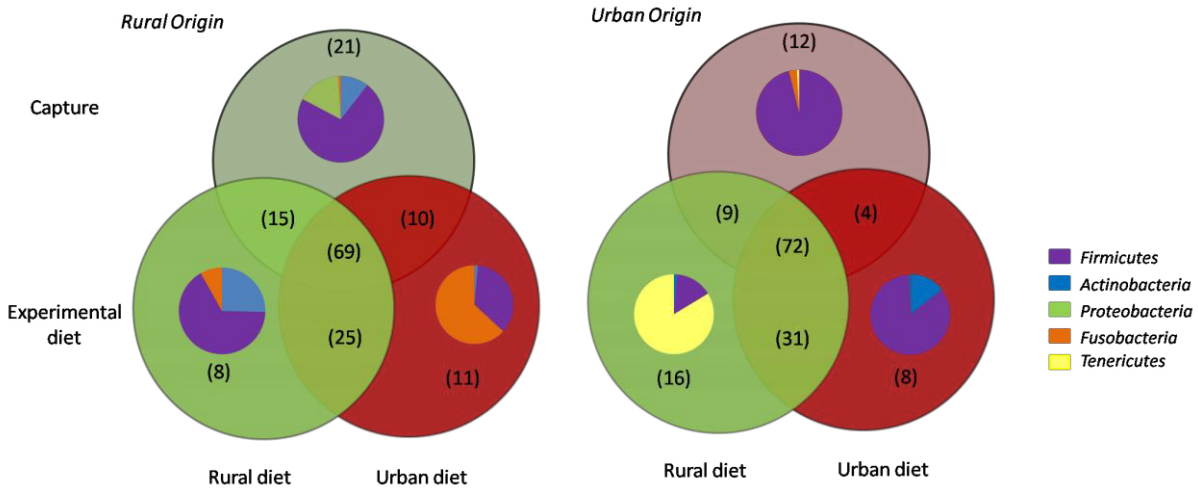

Figure S11: Overlap in gut microbiota communities at capture and after the diet experiment, according to the bird's origin. Numbers in parenthesis refer to the number of specific OTUs for each category. Pie-charts represent the phyla abundance of the specific unique OTUs. Venn diagrams t were calculated based on communities where each OTUs were at least present in 10% of the individuals for each groups.

Supporting tables

Table S1: Summary of the Adonis results based on Jaccard (presence-absence) dissimilarity matrices

	$F_{1,193}$	R^2	p-value
Captivity	13.35	0.064	0.001
Diet	2.05	0.01	0.001
Origin	2.2	0.01	0.002
Captivity*Diet	2.42	0.011	0.001
Captivity*Origin	3.34	0.016	0.001
Diet*Origin	1.38	0.006	0.06
Captivity*Diet*Origin	1.19	0.006	0.17

Table S2: Summary of the Adonis results based on family-binned Jaccard (presence-absence) dissimilarity matrices

	$F_{1,110}$	R^2	p-value
Urbanisation	3.62	0.03	0.002
Capture site	3.20	0.13	0.001

Statistical models

```
library(vegan)
library(nlme)
library(smatr)
library(lme4)
library(reshape)
library(lmerTest)
```

1. *Scale mass index (SMI)*

```
for.slope <- sma(log(weight) ~ log(tarsus length))
bSMA<- unlist(for.slope$coef)[2]
L <- mean(na.omit(tarsus length))
smi<- weight*((L/ tarsus length)^bSMA)
```

2. *global models on α-diversity indices*

```
lme(logOtuRichness~origin*diet*time+sequencing depth, random=~1|bird ID,data=div_indices)
lme(logShannon~origin*diet*time+sequencing depth, random=~1|bird ID,data=div_indices)
lme(logChao~origin*diet*time+sequencing depth, random=~1|bird ID,data=div_indices)
```

3. *models on α-diversity indices at capture*

```
lme(logOtuRichness~origin*sex*age*SMI+sequencing depth,
random=~1|capture_site,data=div_indices_capture)
lme(logShannon~origin*sex*age*SMI+sequencing depth,
random=~1|capture_site,data=div_indices_capture)
lme(logChao~origin*sex*age*SMI+sequencing depth,
random=~1|capture_site,data=div_indices_capture)
```

4. *models on α-diversity indices post-experiment*

```
lme(logOtuRichness~origin*diet*sex*age*SMI+sequencing depth, random=~1|cageID,
data=div_indices_post_experiment)
lme(logShannon~origin*diet*sex*age*SMI+sequencing depth, random=~1|cageID,
data=div_indices_post_experiment)
lme(logChao~origin*diet*sex*age*SMI+sequencing depth, random=~1|cageID,
data=div_indices_post_experiment)
```

5. *models on SMI, mass gain post-experiment*

lme(SMI~origin*diet*sex*age* α-diversity indexes +sequencing depth,
random=~1|cageID/birdID, data=body_condition _post_experiment)

lme(mass_gain~origin*diet*sex*age* α-diversity indexes +sequencing depth,
random=~1|cageID/birdID, data=body_condition _post_experiment)

6. β-diversity analyses

pa_community<-decostand(community, method="pa")

similarity_matrice-pa<-vegdist(pa_community,method="Jaccard")

abundance_community<-decostand(community, method="Hell")

similarity_matrice_abundance<-vegdist(pa_community,method="Bray")

adonis2(similarity_matrice-pa ~time*origin*diet,by="margin",permutations=1000)

adonis2(similarity_matrice-abundance ~time*origin*diet,by="margin",permutations=1000)